Considerations on the Dwell Time for a Vibrating Intrinsic Reverberation Chamber

Danilo Izzo[1,2]
[1]THALES Germany
Ditzingen, Germany
d.izzo@utwente.nl

Robert Vogt-Ardatjew
[2]University of Twente
Enschede, The Netherlands

Frank Leferink[2,3]
[3]THALES Nederland B.V.
Hengelo, The Netherlands

***Abstract*— The dwell time is an important factor when conducting a radiated immunity test and shall be compatible with the response time of the device under investigation. In mode-stirred reverberation chambers, like the vibrating intrinsic reverberation chamber, the electromagnetic field is continuously stirred by the flexible, vibrating walls of the cavity and the time duration of high-strength interferences is generally unknown. Therefore, concerns have arisen regarding the proportion of time that the electromagnetic field level spends at or above the target level during the test. This study investigates, through empirical and simulated data, the expected value of this time interval, considering a threshold level equals to the quantile-80% of the field samples distribution. This information is useful for the user of the method, when considering a mode-stirred reverberation environment for devices with a well-known response time.**

Keywords—vibrating intrinsic reverberation chamber, VIRC, reverberation chambers, dwell time.

I. INTRODUCTION

Any electronic system shall be tested against an external electromagnetic field in order to determine if a susceptibility problem, in presence of such a field, can occur. The possible failures of a device under test (DUT) can be induced by the energy coupled to the victim circuit by an external electromagnetic field [1]. The radiated immunity (RI) assessment, performed to find eventual susceptibility problems to external, radiated electromagnetic fields, can be characterized though three parameters: The electric field strength, the field polarization (typically only horizontal and vertical) and the minimum application time of the stress signal (the dwell time). In particular, the length of the dwell time is determined by the characteristic response time of the DUT, which depends on several factors like the clock frequencies or the specific field of application for which the DUT is designed. However, the choice of the dwell time determines the total test time and the validation responsible shall make a compromise between a dwell time that is technically desirable (large enough to observe a failure) and economically viable (short enough to contain the costs). Furthermore, a relative long temporal window (e.g. 2 s) can be considered enough to determine a failure condition but the limited time allocated for the electromagnetic compatibility (EMC) test activities may limit the number of set-up (i.e., position and orientations of the DUT) one can consider for the validation. When performing the radiated susceptibility test, it is also important considering that the nature of the external electromagnetic interference, is generally not deterministic, i.e., the noise signal received at the DUT does not contain only a direct, constant line-of-sight radio disturb (if present), but also a large number of reflected ones that determine a circular Gaussian electromagnetic field [2]. This is a particular statistical electromagnetic field that can be used to model the dynamic of complex electromagnetic environments like an outdoor environment or the ambient interferences that affect the victim circuits and that are randomly generated by nearby, switching electronics [3]. Reverberation chambers (RC) [4] have been shown to be useful tools for the generation of such statistical fields [5]. A further advantage of RCs is that they make, as consequence of the uniformity and isotropy properties of the electromagnetic field, the test result independent from the particular set-up used for the validation [6].

The vibrating intrinsic reverberation chamber (VIRC) was introduced in [7] as alternative resonant environment to RCs and enables faster and cost-effective testing. It implements a mode-stirring in order to reach a uniform density of the interior electromagnetic field. A VIRC was used in [8] to rapidly convert a semi-anechoic chamber into a reverberation environment (called hybrid chamber) or in [9] to perform in-situ measurements. Here the vibrations of the corrugated, flexible walls perform a fast-stirring of the cavity field and the homogeneity and isotropy conditions are obtained in a short time. Though, it was questioned in [10] that when the boundary conditions of the cavity field are changed too fast, one cannot maintain the magnitude (and the polarization) of the electric field level constant for a long time. Actually, a Tunable Intrinsic Reverberation Chamber (VIRC with a mode-tuner) was proposed in [9] but this solution loses the advantages of the fast, mode-stirring action. With a mode-tuned strategy, in fact, the test time is controlled by the rotating stirrer, which shall be moved stepwise for each working frequency. For example, when 12 different angular positions of the stirrer are necessary [11] and a dwell time of 2 s is required, the analysis would take 24 s for each working frequency. The total revolution time of the stirrer can be even larger in the lowest part of the usable frequency range where more samples can be required to satisfy the uniformity and isotropy conditions [11]. Thus, on one side the VIRC offers, with its fast mode stirring, a real advantage in terms of time and costs, but on the other side it cannot maintain the strength level of the electric field constant over a long dwell time. Since, at the best of our knowledge, there are no studies addressing the problem of determining how fast can be a VIRC in changing the boundaries imposed to the internal electromagnetic field, we want now to estimate the temporal length of a stressing condition in a VIRC and compare it with the traditional dwell time definition given for deterministic fields. Thus, we propose and analyze a model where the test levels are determined by the expected quantile-80% as well the maximum of the field sample distribution. Consequently, a stress condition is defined as the interval between those two values. The Fig. 1 shows the variation of an electric field component measured at one corner of the working volume (WV) by a linearly polarized antenna and during the stirring action (the set-up is described in the next section) of a VIRC. Here, it is possible to observe how local maxima are reached only for a few fractions of milliseconds but the strength level can be maintained above the quantile-80% of the sample population hundreds of milliseconds.

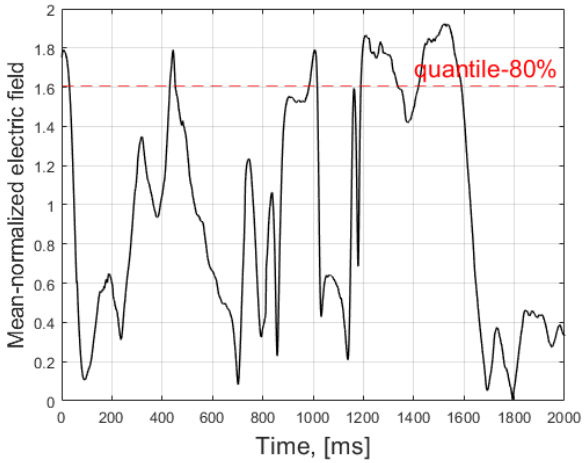

Fig. 1. Rectangular component of the electric field samples measured by a fast field probe in a VIRC. The sample values have been normalized with the dataset mean value.

The paper is structured as follows: the experimental set-up is introduced in Section II and the statistical analysis of the field samples given in Section III. Typical stress conditions are discussed in Section IV and conclusions in Section V.

II. Measurement Set-Up

All experiments were performed in a VIRC installed at the University of Twente (UT-VIRC) [12]. This is a 1.5 m x 1.2 m x 1.0 m rectangular structure whose internal walls are made of conductive material and shacked by two stirring motors positioned at opposite corners of the structure (Fig. 2). According to the simple criterion given in [11], the lowest usable frequency (LUF) of the cavity could be found at three times the fundamental cavity resonance, i.e., 450 MHz. The receiving antenna is a double-ridged horn type directed to a moving wall in a non-line-of-sight configuration with the transmitting discone-antenna. The two antennae were cross-polarized. The receiving antenna has been located, vertically polarized (formally, the z direction), in eight different positions of the WV separated by a minimum distance of $\lambda/2$. The electromagnetic field was sampled with a frequency of 1000 *samples-per-second* (sampling time is 1 ms).

The field uniformity calculation was based on the standard deviation of the value of the local maximum electric field strengths measured by the antenna at the corners of the WV and according to IEC normative equation (1) [11].

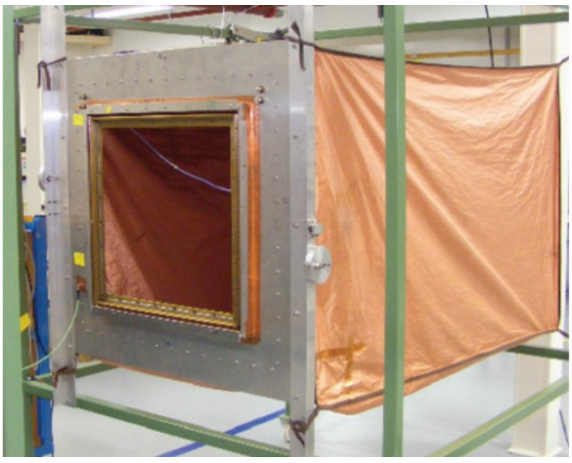

Fig. 2. VIRC installed at the University of Twente.

$$\sigma(dB) = 20\,log_{10}\left(\frac{\sigma + \langle Emax\rangle}{\langle Emax\rangle}\right) \qquad (1)$$

$\langle Emax\rangle$ is the averaged value of the local maxima (averaged in time during the stirring process) and σ their linear standard deviation. In the following sections, the expected quantile-80% value of the sample distribution will be also used in (1).

III. Statistical Description of the UT-VIRC

A. The cumulative distribution function

The Cartesian component of the electric field in a well-stirred RC is a random variable, and its cumulative distribution function (CDF) is Rayleigh-type. The Fig. 3 shows the empirical CDFs for 2000 field samples taken at 2 GHz in eight different measurement positions of the WV vs. the ideal Rayleigh CDF. At 2 GHz, the wavelength is about a tenth of the UT-VIRC´s largest dimension. As soon as the electrically dimensions of the UT-VIRC becomes smaller, i.e., below 1 GHz, the empirical CDFs of Cartesian field samples do not fit the mentioned ideal CDF (Fig. 4). Note that the visual inspection of the CDF curves is not an effective statistical analysis and several hypothesis tests have been proposed in the literature. Here, we just report that the empirical statistical distribution of the Cartesian field samples and its non-idealities can be better described by a two-parameter Weibull distribution when working with electromagnetic fields at frequencies close to the LUF [13].

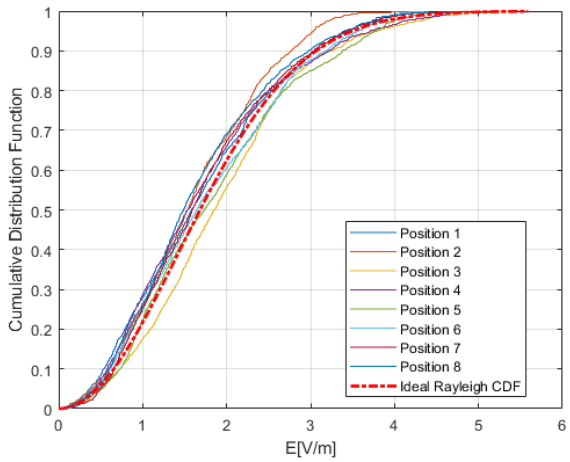

Fig. 3. CDFs of the measured field samples (dataset size is 2000 samples) show agreement at 2000 MHz with the ideal Rayleigh CDF.

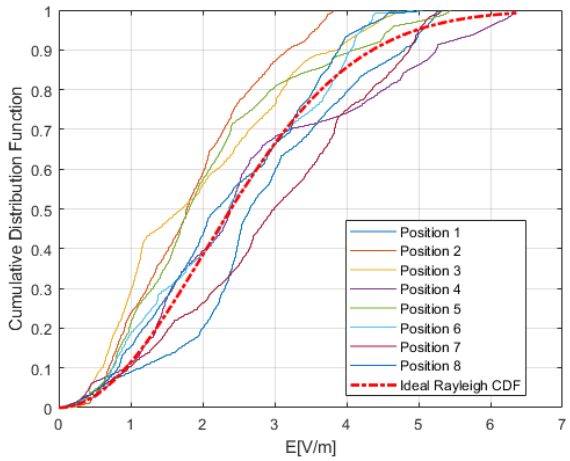

Fig. 4. CDFs of the field samples measured at 600 MHz and for each measuring position. The dataset size is 2000 samples.

Nevertheless, (1) can satisfy the normative rule also in the case that the empirical CDF of the Cartesian field samples is not Rayleigh-like. This is important to understand the reason behind the larger differences between the simulated (based on samples Rayleigh-distributed) and empirical (based on samples Weibull-distributed) results described in the next sections at the lower working frequencies.

B. The coherence time

The autocorrelation function (ACF) has been used to study the coherence time (CT) [8] of the UT-VIRC; this metric gives the largest temporal distance between uncorrelated samples of the electric field strength in a dataset. These uncorrelated values of the electric field have been produced by independent boundary conditions imposed to the electromagnetic field. In other words, the CT measures how long a field strength remains correlated in time or, equivalently, the speed at which the electric field strength changes over a period of time. The estimation of the ACF was accomplished from measurements of the electromagnetic field sampled in time (1 ms) and space (eight measurement positions, with distance larger than λ/2). The Fig. 5 shows the typical CT of the UT-VIRC calculated averaging, in space, the measurements obtained for each position (eight in total) and, in time, using 30 datasets of 2000 samples (2 s). The rotational speed of the motors shaking the VIRC has been maintained constant during the test, the lower value of CT at the higher frequencies can be explained through the fact that the dimensions of the folds in the corrugated walls become electrically larger, therefore more effective, at changing the boundary conditions of the cavity field.

The averaging of the CT values was necessary to reduce the effects of non-idealities present at the lower frequencies where the ergodic assumption of the electromagnetic field samples is not valid [5]. In this case, the differences between the empirical results obtained in different measuring positions or intervals of time could be also large. Fig. 6, for example, shows how the ACF may change according to the observation position: The CT of the signal at 700 MHz varies from about 50 ms, in position 8, to 100 ms, in position 6.

Finally, the expected number of uncorrelated samples in the 2 s time dataset used for the test is given in the Fig. 7.

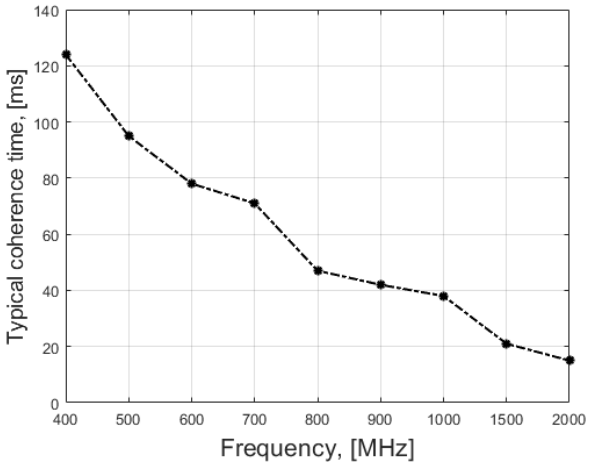

Fig. 5. Averaged value of the cohenrece time (among the eight measurement positions) vs. the working frequency.

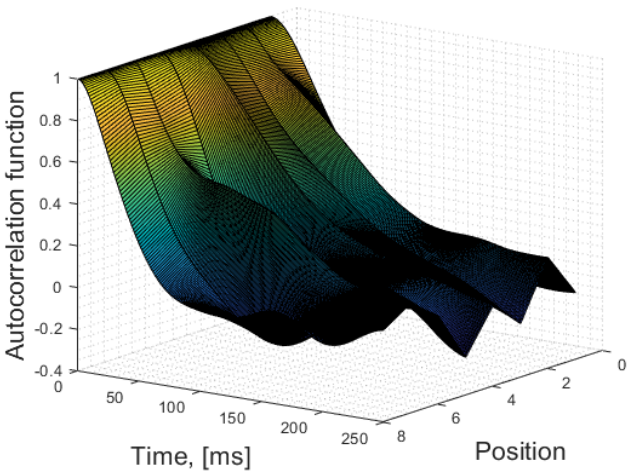

Fig. 6 Autocorrelation function calculated for eight different measurement positions at 700 MHz in 250 ms.

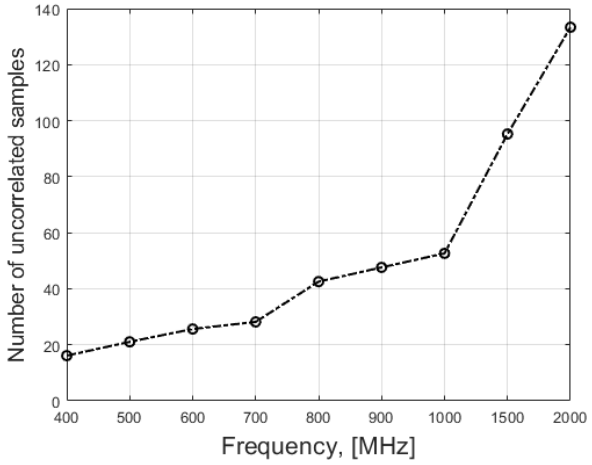

Fig. 7 Expected number of uncorrelated samples in datasets of 2 s vs. the working frequency.

C. The standard deviation

In this section we study the standard deviation of the maximum as well as of the quantile-80% levels for the empirical distributions measured in the UT-VIRC at nine working frequencies from 400 MHz to 2 GHz. The measurement was repeated several times (45 times) to obtain the 95% confidence interval of this indicator.

First, we present a formal definition for the quantile-80% value. Let $e_1, e_2, \cdots, e_n$ be *n* independent measurements of the electric field sampled from a population with a probability density function (pdf) $f(x)$ and CDF, *F(x)*. If *f(x)* is continuous, then α_q is said to be *quantile q* of the distribution if:

$$q = \int_{-\infty}^{\alpha_q} f(x)dx, \qquad (0 < q < 1) \tag{2}$$

Thus, the quantile-80% indicates the value below which the 80% of observations in a group of samples fall. We have used a Monte-Carlo (MC) simulation to compare (1), referred to the maximum and the quantile-80% levels. At each iteration, the program generates eight datasets (to simulate measurements taken at the eight corners of a WV) with variable size and with sample values from a Rayleigh distribution. Fig. 8 shows the 95% confidence interval of the simulated results for datasets of size between 10 and 100.

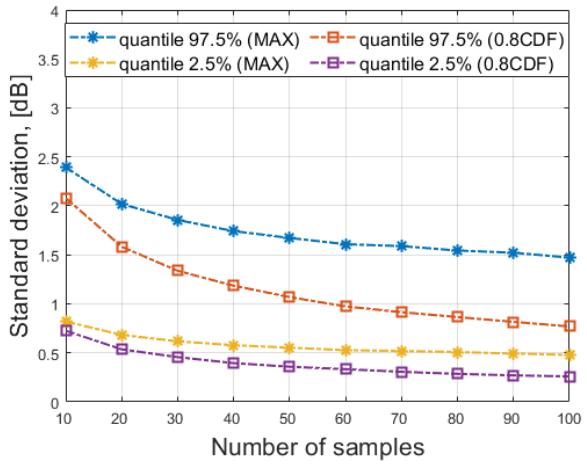

Fig. 8. Typical standard deviation range (95% confidence interval) for the maximum (MAX) and quantile-80% (0.8CDF) values among 10000 iterations of the MC program. The standard deviation is calculated for eight dataset with size (number of samples) of 10 to 100 samples.

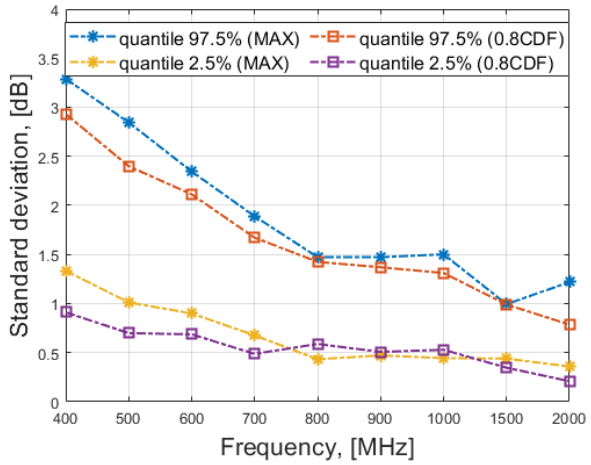

Fig. 9. Typical standard deviation of maximum (MAX) and quantile-80% (0.8CDF) levels into the UT-VIRC. Results refer to a population of 45 independent test and fixed observation time of 2 s.

The experimental results agree reasonably with the simulations, however only where the empirical statistical distribution fits the ideal Rayleigh one. For example, in the empirical data, above 700 MHz, one can find datasets with more than 50 uncorrelated samples (Section III-B), i.e., the expected worst case for the standard deviation is between about 1 dB (for the quantile-80% values) and about 1.5 dB (for the maximum values) (Fig. 8).

The LUF can be positioned at 500 MHz (Fig. 9), where the 95% CI of the estimates of (1) is below 3 dB, despite the use of the quantile-80% in place of the maximum value in (1) would slightly improve its position (from 500 MHz to 400 MHz).

IV. Observations on the Magnitude and Duration of a Stress Conditions

A. The expected overshoot above the threshold level

In this section we describe how the stress level of the test was determined for the UT-VIRC. In particular, we want to characterize a stress condition as the interval of time during which the magnitude of the electric field strength remains above the expected quantile-80% value for a 2 s interval. The statistical characterization of the extreme values in dataset of electric field samples include the generalized extreme value distribution (GEV) based on the extreme value limit distributions first identified by Fisher and Tipp [14] and the generalized Pareto distribution (GEP) [15]. Those theories have been considered to solve the problem of characterizing the tail of a sample distribution in overmoded [16] reverberation chambers. For the sake of simplicity and without the loss of generality we have studied the problem with the help of a Monte-Carlo simulation [17]. The program uses pseudorandom number generator to construct eight datasets of N independent samples according to the known Rayleigh distribution. The value of N, for each working frequency, is given in Fig. 7. Hence, the differences between the magnitude of the observations over the threshold value and the threshold itself were evaluated in dB:

$$expected\ distance\ Max - to - quantile80\% = \max(dB) - quantile80\%(dB) \quad (3)$$

The simulation program created dataset of 10000 estimations of (3) and, for example at 1 GHz (with about 55 uncorrelated samples), it shows that a ratio between maximum and quantile-80% of about 4.5 dB (Fig. 10, red curve) is expected. Finally, the simulated results are compared with the experimental results. In the frequency region where the Rayleigh assumption for the underlying statistical distribution of the Cartesian field samples does not fully hold (below 700 MHz), simulated and real values have larger differences and, in particular, at 400 MHz a difference of +2.4 dB between the empirical and the simulated data has been found. Above 700 MHz a good agreement, between simulated and experimental results, can be found and the overshoot above the threshold ranges from 3.5 dB to 5 dB depending on the working frequency, the dataset size and the number of uncorrelated samples (Fig. 10). Therefore, under the well-stirred conditions, we would expect a difference between the quantile-80% and the maximum values from 3 dB (dataset of 16 uncorrelated samples) to about 5.2 dB (dataset of 135 uncorrelated samples). Lastly, Fig. 10 reveals also the risk when using a VIRC below or close the LUF where the CDFs of the sample distributions may not lie in the domain of attraction of an extreme value distribution function [15]. Here, it has been observed that the extreme values of the electromagnetic field strength may be higher than that expected for datasets of similar size with negative consequences for the test repeatability.

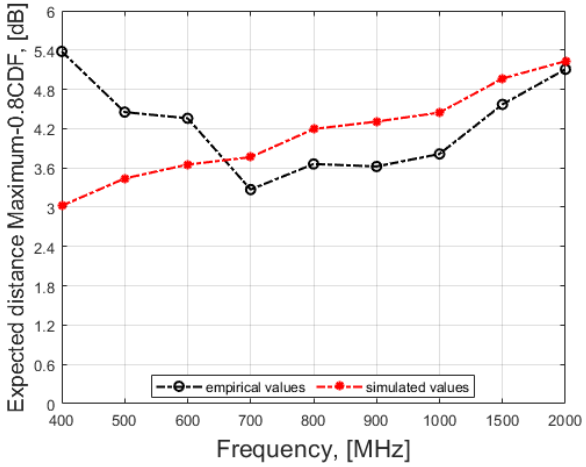

Fig. 10. Simulated (red curve) vs. measured (black curve) values of the distance between the quantile-80% (0.8CDF) and the maximum levels. Measurements refer to avereged data over 45 different test with eight dataset of 2000 samples. The number of uncorrelated samples used for the simulated dataset refers to Fig. 7.

B. *Time Duration of a Stress Condition*

The statistical characterization of the temporal interval in which the electric field strength remains between the quantile-80% and its maximum level, here briefly indicated as a transient (because lasting only a short time), was experimentally determined for the UT-VIRC as follows: Transients were observed for each dataset of 2000 samples (2 s), at eight different positions of the WV and during 45 independent tests. Hence, a total of 360 independent transients have been obtained for each working frequency. Fig. 11 shows their averaged values from 400 MHz to 2000 MHz; note that the temporal length of transients decreases with the increase of the modal density into the resonant cavity. When the modal density is higher, in fact, the CT of the cavity field decreases and the instantaneous rate of change, for the field strength, increases.

The coefficient of variation (CV), i.e., the value of the standard deviation normalized to the statistical mean of the sample datasets was used to determine the spread of the transient values in Tab. I. The advantage of using the CV is that it can compare dataset across different working frequencies which have, typically, different average values (with the same power level transmitted to the cavity). The CV remains stable around 0.3 in the usable spectrum of the cavity from 500 MHz to 2000 MHz; this means that the expected standard deviation on the temporal length of a transient is, for each working frequency, the 30 % of its expected average value. The results obtained show that a typical transient, for example at 1 GHz, is 100 ms long (Fig. 11) and with an expected maximum 3.7 dB above the quantile-80% level (Fig. 10).

TABLE I. STANDARD DEVIATION-TO-MEAN RATIO FOR TRANSIENTS

Frequency [MHz]	Std.Dev-to-Mean
500	0.31
600	0.32
700	0.32
800	0.32
900	0.28
1000	0.32
1500	0.31
2000	0.30

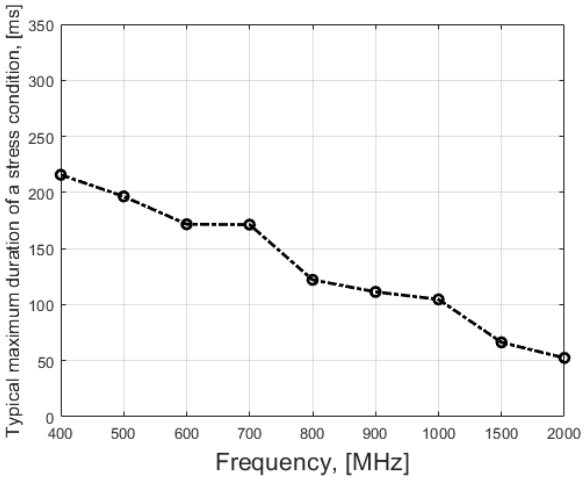

Fig. 11. Typical temporal length of the electromagnetic field strength level above the quantile-80%. The dataset size is 2 s.

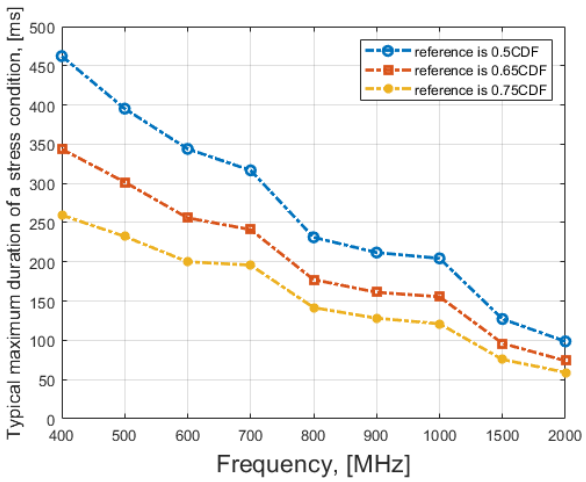

Fig. 12 Typical temporal length of the electromagnetic field strength level above the quantiles-50%,-65% and -75%. The dataset size is 2 s.

Of course, the stress level could be manipulated if one considers a different threshold level. Fig. 12 shows how the expected duration of a transient can be changed with a different choice of the quantile value.

C. *Controlling the Duration of a Stress Condition*

The expected duration of a transient shown in the previous section ranges between 50 ms and 200 ms (Fig. 11). Thus, the total energy of a stressing signal is still a small fraction of the testing energy used with a deterministic field (i.e., created in semi- or full-anechoic chamber) during a dwell time of 2 s. On the other hand, the test operator has some possibilities to regulate the temporal length of transients, which can be controlled by the threshold level (Section IV-B) or by carefully selecting the rotational speed of the motors used for shaking the flexible walls of the VIRC. This follows the fact that the faster the boundary conditions are changed, the smaller is the temporal correlation between consecutive sample values of the electromagnetic field. In this way, one can try adjusting the total length of stress conditions, according to the response time of the DUT. Fig. 13 shows how was possible to regulate the expected value of a transient only by setting different values for the rotational speed of the shaking motors.

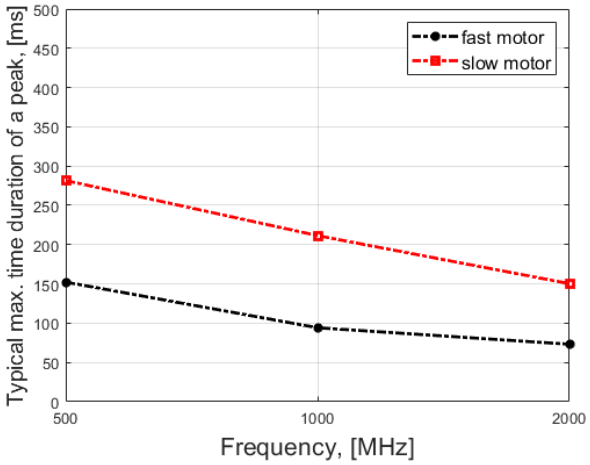

Fig. 13 Typical temporal length of the electromagnetic field strength level above the quantile-80%. Measurement taken for three working frequencies and in two configurations: VIRC shaked by one motor with fast (black curve) and slow (red curve) rotational speed.

V. CONCLUSIONS

We have analyzed in the time domain and with the help of empirical and simulated measurements, the electromagnetic noise generated in a VIRC. In particular, with the definition of a threshold level based on the estimated population quantile (the quantile-80%), a statistical analysis of the temporal length of a stress condition in a VIRC was possible. This temporal length varies, within a dwell time of 2 s, from 50 ms (in the upper part of the usable frequency range) to 200 ms (close to the LUF). Finally, it has been observed that the typical length of electromagnetic field strength above the threshold can be partially regulated through the opportune choice of the quantile level and the speed of the motors shaking the VIRC.

REFERENCES

[1] C. R. Paul, Introduction to Electromagnetic Compatibility, Wiley, 2006.

[2] Q. Xu and Y. Huang, Anechoic and Reverberation Chambers: Theory, Design, and Measurements, Wiley-IEEE Press, 2018.

[3] L. R. Arnaut, "Statistical distributions of dissipated power in electronic circuits immersed in a random electromagnetic field," *Radio Science,* vol. 40, 2005; DOI: 10.1029/2004RS003174.

[4] R. Serra, A. C. Marvin, F. Moglie, V. M. Primiani, A. Cozza, L. R. Arnaut, Y. Huang, M. O. Hatfield, M. Klingler and F. Leferink, "Reverberation chambers a la carte: An overview of the different mode-stirring techniques," *IEEE Electromagnetic Compatibility Magazine,* vol. 6, no. 1, pp. 63 - 78, 2017; DOI: 10.1109/MEMC.2017.7931986.

[5] P. Corona, G. Ferrara and M. Migliaccio, "Reverberating chambers as sources of stochastic electromagnetic fields," *IEEE Transactions on Electromagnetic Compatibility,* vol. 38, no. 3, pp. 348 - 356, 1996; DOI: 10.1109/15.536065.

[6] R. D. Leo and V. Primiani, "Radiated Immunity Tests: Reverberation Chamber vs. Anechoic Chamber Results," in *2005 IEEE Instrumentationand Measurement Technology Conference Proceedings*, Ottawa, Ont., Canada, 2005; DOI: 10.1109/IMTC.2005.1604130.

[7] F. Leferink, J.-C. Boudenot and W. v. Etten, "Experimental results obtained in the vibrating intrinsic reverberation chamber," in *IEEE International Symposium on Electromagnetic Compatibility.*, Washington, DC, USA, 2000; DOI: 10.1109/ISEMC.2000.874695.

[8] D. Izzo, A. Rommel, R. Vogt-Ardatjew and F. Leferink, "Validation and Use of a Vibrating Intrinsic Reverberation Chamber for Radiated Immunity Tests," in *2020 IEEE International Symposium on Electromagnetic Compatibility & Signal/Power Integrity (EMCSI)*, Reno, NV, USA, USA, 2020; DOI: 10.1109/EMCSI38923.2020.9191603.

[9] F. Leferink, "In-situ high field strength testing using a transportable reverberation chamber," in *2008 Asia-Pacific Symposium on Electromagnetic Compatibility and 19th International Zurich Symposium on Electromagnetic Compatibility*, 2008; DOI: 10.1109/APEMC.2008.4559891.

[10] P. Corona, J. Ladbury and G. Latmiral, "Reverberation-chamber research-then and now: a review of early work and comparison with current understanding," *IEEE Transactions on Electromagnetic Compatibility,* vol. 44, no. 1, pp. 87 - 94, 2002; DOI: 10.1109/15.990714.

[11] IEC 61000-4-21, Electromagnetic compatibility (EMC) - Part 4-21: Testing and measurement techniques - Reverberation chamber test methods, 2011.

[12] R. Vogt-Ardatjew and F. Leferink, "Observation of maximal and average field values in a Reverberation chamber," in *2013 International Symposium on Electromagnetic Compatibility*, Brugge, Belgium, 2013.

[13] C. Lemoine, P. Besnier and M. Drissi, "Investigation of Reverberation Chamber Measurements Through High-Power Goodness-of-Fit Tests," *IEEE Transactions on Electromagnetic Compatibility ,* vol. 49, no. 4, pp. 745 - 755, 2007; DOI: 10.1109/TEMC.2007.908290.

[14] G. Orjubin, "Maximum Field Inside a Reverberation Chamber Modeled by the Generalized Extreme Value Distribution," *IEEE Transactions on Electromagnetic Compatibility,* vol. 49, no. 1, pp. 104 - 113, 2007; DOI: 10.1109/TEMC.2006.888172.

[15] J. Pickands, "Statistical Inference Using Extreme Order Statistics," *The Annals of Statistics,* vol. 4, no. 1, pp. 119-131, 1975.

[16] J. Kostas and B. Boverie, "Statistical model for a mode-stirred chamber," *IEEE Transactions on Electromagnetic Compatibility ,* vol. 33, no. 4, pp. 366 - 370, 1991; DOI: 10.1109/15.99120.

[17] J. Ladbury, "Monte Carlo simulation of reverberation chambers," in *Gateway to the New Millennium. 18th Digital Avionics Systems Conference*, St Louis, MO, USA, USA, 1999; DOI: 10.1109/DASC.1999.822102.